



Contract No. 212206

Cost-Effective

Resource- and Cost-effective integration of
renewables in existing high-rise buildings

SEVENTH FRAMEWORK PROGRAMME
COOPERATION - THEME 4
NMP-2007-4.0-5 Resource efficient and clean buildings
Grant Agreement for: Collaborative Project
(ii) Large-scale integrating project

D3.3.2 Description of prototype for BIPV component

Due date of deliverable: month 30

Actual submission date: 15/03/2011

Start date of project: 01/10/2008

Duration: 48 months

Organisation name of lead contractor for this deliverable: [Fraunhofer ISE](#)

[Revision 9.7.2009](#)

Project co-funded by the European Commission within the Seventh Framework Programme (2007-2013)		
Dissemination Level		
PU	Public	X
PP	Restricted to other programme participants (including the Commission Services)	
RE	Restricted to a group specified by the consortium (incl. the Commission Services)	
CO	Confidential, only for members of the consortium (incl. the Commission Services)	

Contents

1	Introduction	3
2	Characteristics and properties	5
2.1	Technical description	6
2.1.1	Definition of the γ -angle	9
2.1.2	Definition of the ϕ -angle	9
2.2	Geometry optimization	10
3	Production of first functional models	13
3.1	Laboratory measurement	14
3.1.1	Angles-dependent transmittance at Fraunhofer ISE	14
4	Simulation Analysis	17
4.1	Static simulation	17
4.2	Daylighting availability	18
4.3	Glare protection	20
4.4	Building energy simulation analysis	21
5	PV Integration	24
5.1	Current available thin-film PV technologies	24
5.2	BIPV potentiality	26
5.2.1	First evaluation of the efficiency	27
6	Façade Integration	30
7	First Prototype	32
8	References	33

Author

Head of Group Solar Facades

Dr. Ing. Francesco Frontini

Dipl. Phys. Tilmann E. Kuhn

1 Introduction

Many recent researches attest that the 40% of the European energy consumption is due to the building. In particular the 80% of building energy consumption currently occurs during service-life. The energy used for cooling is raising day by day, and also the energy for heating and for lighting [13].

Nevertheless, it has been attested that all the building, residential or commercial, have an enormous potential for improving the energy efficiency (think about the standard passive-house in Germany and Austria) and of energy systems integration, like pv-systems or solar cooling systems, to produce energy from the sun. This is particularly true for non-residential sector and high-rise buildings.

The European-parliament adopted an own-initiative report on a roadmap for renewable energy in Europe which calls on the Commission to present, by the end of 2007 at the latest, a proposal for a renewable energy legislative framework. Parliament calls on the Commission to ensure that the forthcoming legislative proposal concerning renewable energies contains strong measures for the promotion of renewable electricity, with the aim of increasing its share in the EU from the present level to at least double that amount by 2020 (A roadmap for renewable energy in Europe, 25-09-2007 [8]).

In façade construction, in particular for high-rise buildings, the portion of the glazed area of the façade rises continuously. The architects like very much transparency, the sun and the contact with the city and the context.



Figure 1: Systems Integration in building. Source: 1) BEAR Architects, 2) Viessmann, City of Tomorrow in Sweden, 3) Viessmann, University of Stuttgart.

This causes the positive effect of higher daylighting for the internal space and reduction of energy consumption for artificial lighting but, on the other hand, produces the risk of overheating, in particular during summer period and/or high cooling loads. For that reason, sun protection is necessary.

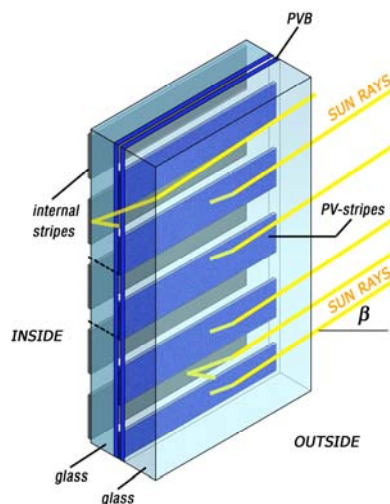
It is very common in Central or North Europe to control the solar gains with external shading systems (for example venetian blinds). This solution has some advantages for residential house (family houses), because of the high efficiency and the low cost of installation, but on the other hand venetian blinds doesn't produce energy (no electricity production) and are not suitable for high-rise buildings and windy locations.

The new angle selective pv-façade, presented in this report, combines in one-element four important tasks: solar protection, glare protection, visual contact and integrated pv-system for electricity production. These four elements, as are completely integrated in the function of the façade, do not reduce the architectural goal of the glazed façade and the view from the interior to the exterior is guaranteed.

2 Characteristics and properties

The new angle-selective-façade system is at the same time a static sun protection façade and a solar electricity generator, which can be produced using the usual production technologies of windows and glazing units. It is also possible to use stripes made from other material than PV-cells. The particular position of the stripes and the different refraction index of glass and air are the physical and optical properties that permit the protection against sun and that prevent the occupants against glare.

The stripes should be opaque and can be in different material or colours, depending on the architectural idea and shading and energy generation requirements.



They could be completely black to maximize the shading and anti-glare performance or red, blue or what colour the architect needs for his aesthetic purpose. The invention can be implemented with or without photovoltaic strips in the outer and/or inner part, depending on the purposes, to produce electricity. The main purpose within the project Cost-Effective is to develop a solution that uses PV-cells for the outer and maybe also for the inner stripes.

How it works:

- Solar protection: the sun is blocked and faded out starting from a certain angle (γ^*) that is related to the solar altitude angle. A certain part of sunrays is stopped and reflected or absorbed (depending on the colour and on the material of the stripes) by the external series of stripes (generally rays with an incident angle greater than γ); the other rays are blocked by the internal series of stripes.
- Glare control: the opaque stripes selectively shield certain region of the sky, which means that people are protected against the very high luminance ($>10^9$ cd/m²) of the direct sun.

- Electricity production: different kind of PV-technologies could be used as opaque stripes to produce electricity from the sun.

2.1 Technical description

For a vertical façade facing to the south, the stripes are preferably horizontal.

For different orientations the strips should be turned in according to the illustration ([Figure 2](#)), to maximize the solar protection and glare.

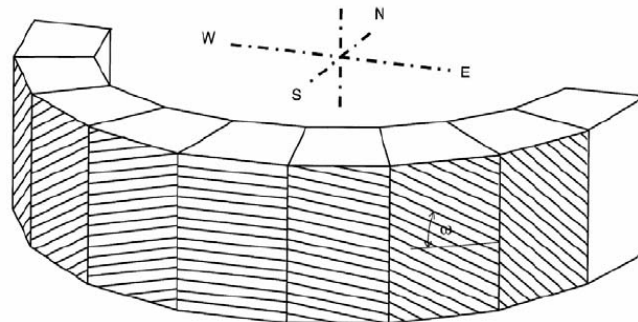


Figure 2: The inclination angle ω of the ribs relative to the horizontal within the window plane for different window directions (source Lorenz [6]).

The inclination ω of the stripes depends on the latitude of the site, on the orientation of the façade and on the inclination of the façade.

The basic idea is to shield only the angle greater than a defined γ -angle and leave the view transmission from the inside, independent from the view angle ϕ .

[Figure 3](#) shows the difference between the basic idea, where the γ angle is defined as 20° and the critical angle ($\approx 41^\circ$) is assumed for the design of the stripes and the façade, and the optimized design of the new-façade. The differences are in the positions of the point two and of the point four.

To optimize the basic idea, two independent parameters are introduced to control and calculate the internal view transparency (χ and α). These two parameters and other three variables, related to the solar transmission and optical characteristics, represent the variables used for defining and optimising the new-system.

The parameters take into account also the position of the sun and the latitude of the site in where the façade will be installed. The following image explains the angular selective façade characteristics.

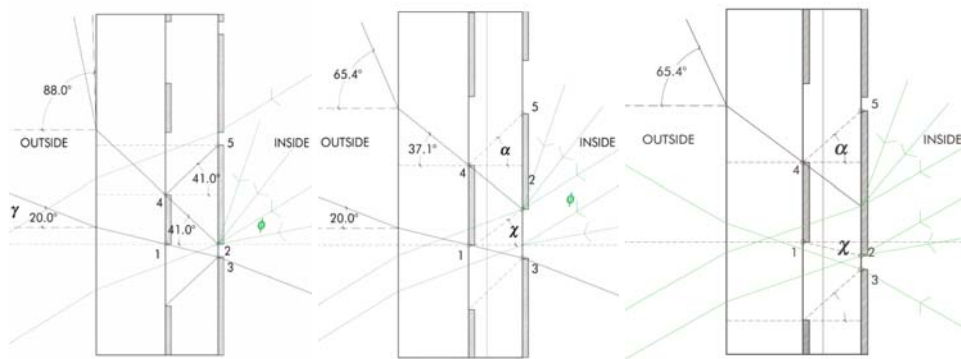


Figure 3: The basic idea (on the left side) has an internal view transmission independent from the view angle ϕ . The two pictures on the right take into account the new parameters. The view transmission from the inside is higher and depends on the view angle ϕ .

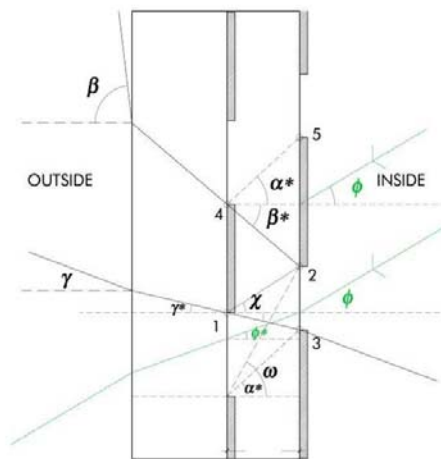


Figure 4: Description of the parameters. Two independent parameters are introduced to optimize the system: χ, α

Table 1: Definition of the variables (the angles are positive if they are clockwise and negative anti-clockwise, the lengths are always considered positive)

α	Max Internal view angle	$\alpha < \text{critical angle } (\approx 42^\circ)$
β	Max shadowing angle	Depends on max solar altitude
γ	Min shadowing angle	Depends on solar altitude (in the present work 20° is taken as min angle).
χ	Transparency variable (so called by the authors)	Defines the position of the internal stripe in relationship to the external ones.
ϕ	Internal view angle	It is referred to the position of the eyes of the occupant.
s	Internal glass pane thickness	2mm – 8mm
$\bar{\cdot}^*$	Represent the refracted ray due to the Snell law	$\left(\frac{\sin \alpha_1}{\sin \alpha_2} = \frac{n_2}{n_1} \right)$ where $n_1 \approx 1$ (air) and $n_2 \approx 1.52$ (glass)
\bar{DH}	Dimension of the internal stripe	$\bar{DH} = s \cdot (tg\alpha - tg\beta^*)$
\bar{DB}	Internal transparent stripe	$\bar{DB} = \bar{DO} + \bar{OB} = s \cdot (tg\chi - tg\gamma^*)$
\bar{GF}	Dimension of the external stripe (between the two glass panes)	$\bar{GF} = \bar{ED} + \bar{DO} = s \cdot (tg\chi - tg\beta^*)$
τ	Visual Transmission of the system	

To completely define the geometry, four steps are needed:

- Define the minimum angle to shadow (γ).
- Define the transparency independent variable (χ).
- Define the solar altitude by:

$$\sin(Alt) = \cos(Lat) \cdot \cos(Decl) \cdot \cos(Hangle) + \sin(Lat) \cdot \sin(Dec)$$

Where:

Alt	=	Altitude
Lat	=	Latitude
Decl	=	Declination
Hangle	=	Hour angle

- Last step is to define the dimension of the internal stripe defining α^* .

2.1.1 Definition of the γ -angle

The γ -angle is related to the minimum shadow angle and the minimum angle of glare protection. This angle is also related to the maximum solar energy transmission: the energy transmission of the system increases together with the γ -angle.

The purpose of the new façade is to leave the maximum solar energy outside during the summer period and to guarantee a certain amount of solar gain during the cold season. For this reason a compromise must be accepted: large values of γ gives larger solar gains, with consequently increasing the cooling demand in summer period, better transparency, less glare protection and lower heating power demand in winter.

To have good solar gains during winter the angle of $\gamma = 20^\circ$ from the horizontal is assumed.

During the summer period, the solar altitude and the profile angle are higher than in winter. In Freiburg (Germany), the solar altitude is always below 64° .

2.1.2 Definition of the ϕ -angle

For the optimization of the view contact to the exterior, the more frequent positions of the occupant in the room must be taken into account. This influences the angle of internal view and the position of the stripes.

In the present report, an office with the following dimension is taken into account:

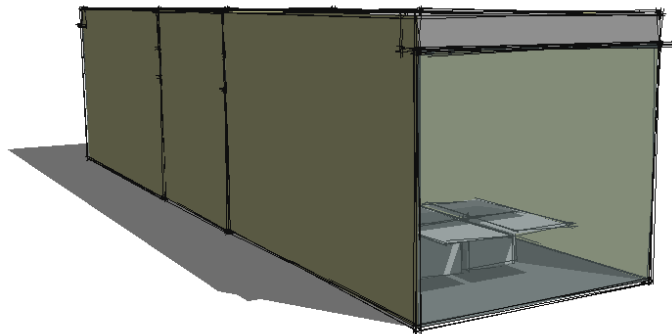


Figure 5: The Office model.

Table 2: Size of the considered office.

Model	Gross Volume	Net Floor Area	Height	Transparent Area
A	60.62 m ³	18.37 m ²	3.3 m	11 m ²

The occupant frequently stays far from the façade about one or two meter, this means that the angles of internal view are between -20° and 35° , position at 1 meter from the window. If point B will be considered is $-20^\circ \leq \phi \leq 35^\circ$ (see [Figure 6](#)).

Consequently, it is possible to understand (see [Figure 6](#)) how the view angles stay, more frequently, in a range between -20° (looking up to the sky) and 35° (looking down).

The angles that are higher than 35° are excluded because the occupant must be very close to the façade looking down, a condition that is uncommon for office spaces or big open spaces.

In [Figure 6](#) the situations A and A' represent one person standing or sitting 1,00m close to the window looking outside, the configurations B and B' represent the eyes of an occupant standing and sitting near the façade 2,00m. The point C is the situation of a person close to the door (2,50m from the window) that is looking directly to the façade.

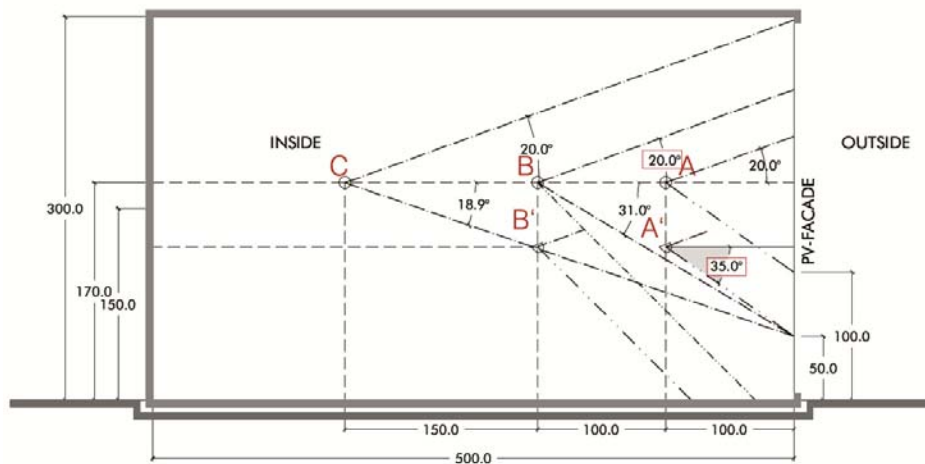


Figure 6: The image represents the scheme of the internal view angle for an occupant sitting or standing at 1m or 2m from the window and an occupant standing at 3,5m from the window. The angle range is 20° (up-view) to 25° (down-view). The most probable angles are between $-20^\circ < \phi < 35^\circ$.

2.2 Geometry optimization

A first optimization of the system has been done to reach the best glare protection and the highest visual transmission from the inside to the outside. Another optimization is currently in progress in order to optimize the electricity production performances (pv-integration).

In this first step the visual transmission (τ_{vis}) has been calculated only considering the direct raytrace, this means that no interreflections are considered. This assumption is correct when only visual rays are considered.

The optimization is done according to the most probable occupant position (Figure 6) considering different internal view-angles between $-20^\circ \leq \phi \leq 35^\circ$. The two main variables of the system are the two independent parameters introduced by the author to control the geometry design of the new angle selective façade: α, χ

The refractive indexes of the materials are:

- Air refraction index = 1;
- Glass refraction index = 1.52.

The maximum transmission for a defined internal view angle (ϕ) is reached for an angle selective façade with $\alpha \equiv \chi$ (Figure 7), this means that the internal and the external stripes have the same dimension.

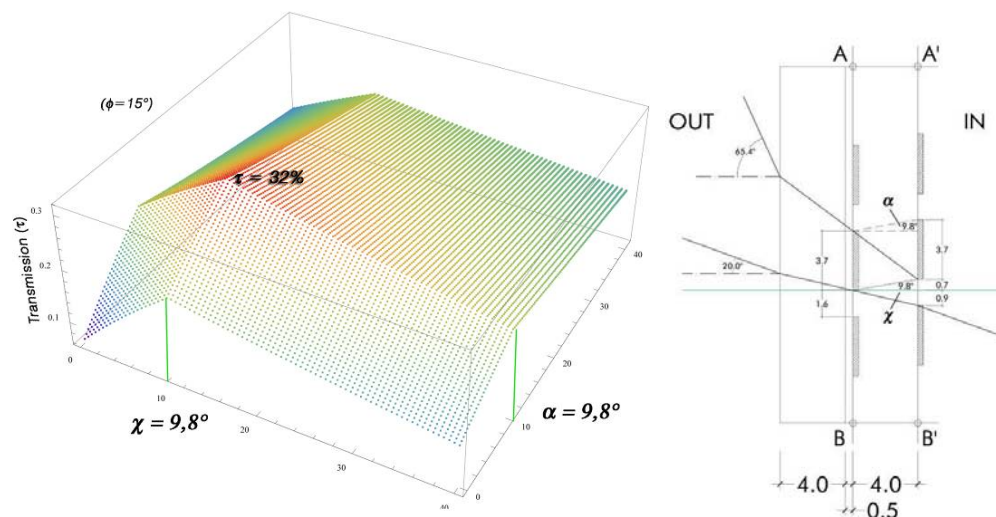


Figure 7:

In this 3D-graph the transmission τ_{vis} depending on the two independent parameters χ and α for the internal view-angle $\phi = +15^\circ$ is plotted. The symmetry of the geometry: $\chi \equiv \alpha$ is also shown. The maximal transmission is $\tau_{max} = 32\%$, reachable for $\chi = \alpha = 9.8^\circ$.

The integration over the more probable view angles $-20^\circ \leq \phi \leq 35^\circ$ for the configuration of $\chi = \alpha$ reveals that the maximal visual transmission (τ) is obtained for $\chi \cong 18^\circ$.

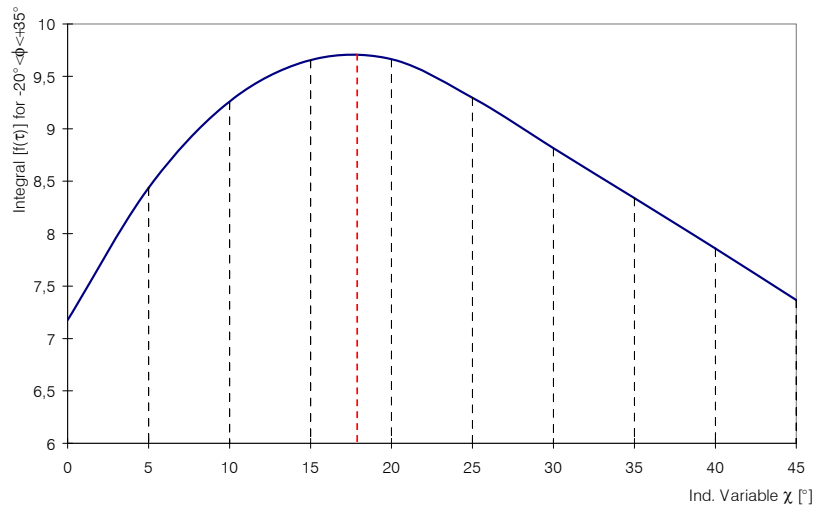


Figure 8: With $\gamma = 20^\circ$ and with $\chi = \alpha$ the maximum visual transmission in the range of $-20^\circ \leq \phi \leq 35^\circ$ is achieved with the value of $\chi \cong 18^\circ$.

The internal stripes and the external stripes are 4,4mm large and the transparent gap between one stripe and the following one is about 2,2mm (Figure 9).

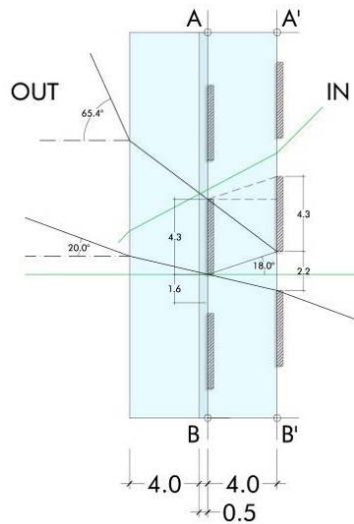


Figure 9: The picture shows the optimized geometry to achieve the best visual transmission from the inside to the outside for the range of $-20^\circ \leq \phi \leq 35^\circ$.

3 Production of first functional models

To validate the mathematical model and the further RADIANCE simulation a first prototype was realized in collaboration with a Cost-Effective project partner Interpane. This first prototype helps the authors to understand the contribution and the potential of the new component. It is always very important to check with real objects what is studied theoretically.

The production of the prototype is done with the current available technology. Laminated glass pane are used. The stripes are fritted on it.

Table 3: Description of the prototype.

PROTOTYPE numb. 1	
Dimension: 1 meter X 1 meter	
Glass thickness	4mm + 4mm
Internal Stripes	5,1mm
External Stripes	4,8mm
Internal stripes-gap	1,9mm+ 0,9mm
External stripes-gap	3mm

In the following pictures show the dependency of the visual transmission (τ) to the angle of view (ϕ) is shown.

Figure 10 shows the prototype if it is tilted with different angles. In the first picture on the left the glass is tilted about $\phi_1 = -30^\circ$ (as the occupant is looking down), in the middle the sample is placed vertically ($\phi_2 = 0^\circ$) and the picture on the right shows the prototyped tilted with an angle more than $\phi_3 > 20^\circ$. The transmission is higher for the position on the left.



Figure 10: Photos of the first prototype. The angular dependency transmission is shown tilting the prototype from -30° (very high transmission) to $+30^\circ$ (the façade is more or less opaque).

The photos in **Figure 11** show the detail of the printed stripes and the appearance of the new angular selective façade if placed as window. The visual contact is really good if we stay 2-3 m away from the glass.

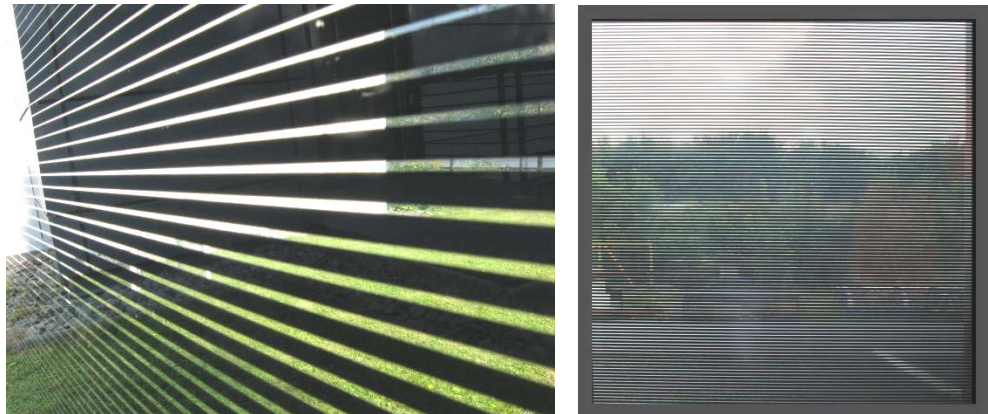


Figure 11: Detail of the stripes and see through picture.

In the next chapter several simulations are shown to evaluate the performances of the new angle selective façade. First the visual contact to the outside is simulated; secondly the daylight contribution and the glare protection are verified. Finally the solar protection is evaluated to attest the impact of the new system in the building energy simulation.

3.1 Laboratory measurement

To determine the real properties of the first example, physical and optical measurements were carried out in the Laboratory of the Fraunhofer ISE. This laboratory is accredited for τ , ρ , g-value and u-value measurements according to DIN EN ISO IEC 17025.

Three different measurements have been carried out:

- Transmission analysis,
- Diffuse reflectance,
- Direct and global reflectance.

The first two measurements are carried out using the Ulbricht Sphere and the second one with the Lambda-900 spectrometer.

3.1.1 Angles-dependent transmittance at Fraunhofer ISE

The angle-dependent solar transmittance and light transmittance τ_{dh}^S and τ_{dh}^L have been determined with an integrating sphere (a simple scheme of the utilized instrument is shown in [Figure 12](#)) using a radiometric detector and a photometric detector. The polar angle ϕ (incidence angle) has been varied from 0° to 75° in steps of 5° .

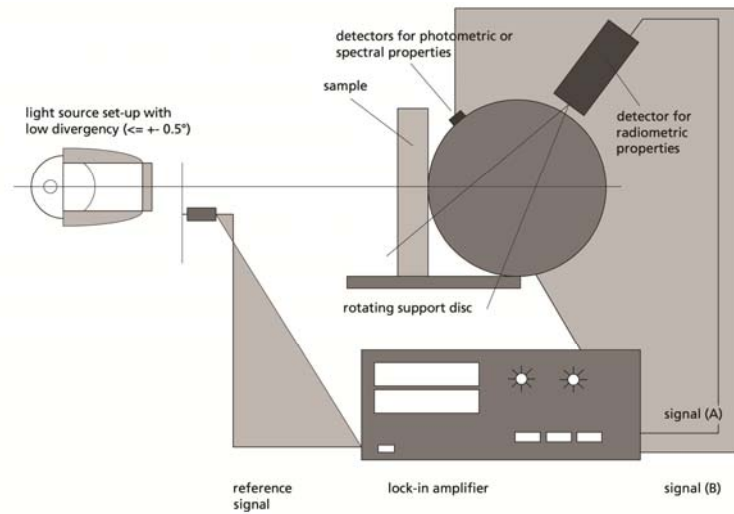


Figure 12: Scheme of the Tau-win instrument in Fraunhofer ISE Laboratory.

The hemispherical reflectance ρ_{hh} of the back side of the samples for incident diffuse radiation (originating from the integrating sphere) has been determined for the samples with the Diffuse Radiation Source DRS using a sample port aperture of 10cm diameter; this value is needed for the second order correction stemming from the change of sphere throughput due to the sample at the measurement port.

The laboratory measurements are carried out twice, with the same configuration, to check the consistency of the results.

The photos in [Figure 13](#) show the laboratory instruments and the installation of the prototype in front of the Ulbricht Sphere.

The angular dependent transmission of the new façade is shown in [Figure 14](#). The measurements are carried out with an integrating sphere. The sample is placed in front of the Ulbricht sphere and is irradiated by parallel light. The sample is tilted every 5° (from -50° to $+75^\circ$) to calculate the transmission. The negative angles represent the direct sunray position.

The maximum transmission is reached for an angle of incident about 35° from below the horizon. The light is blocked, because of the design, for angles higher than 20° above the horizon (20° represents the minimum shadow angles of the system).



Figure 13: The images show the measurements in the Laboratory of Fraunhofer ISE. The first picture on the left represents the sample placed in front of the Ulbricht Sphere.

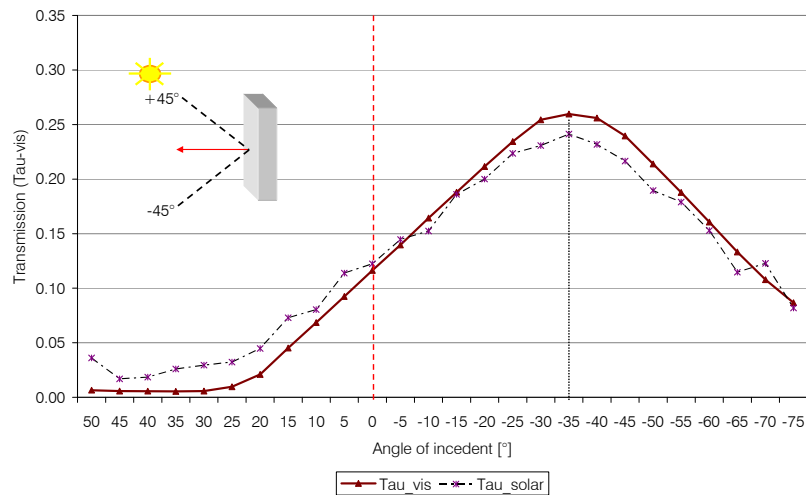


Figure 14: Visual and solar radiation transmission. The measurements are carried out using the integrating sphere with radiometric detector and photometric detector.

The validation of the Radiance model was done with the obtained measured data.

4 Simulation Analysis

The calculation of the daylighting conditions and the visual impression was done with the raytracing software package named RADIANCE [5].

RADIANCE is developed as a research tool for predicting the distribution of visible radiation in illuminated spaces by the Laurence Barkley National Laboratory. Several extensions of the program have been developed by Fraunhofer ISE (e.g. PHOTONMAPPING, DAYSIM and EVALGLARE) The programme uses as input a three-dimensional geometric model of the physical environment, and produces a map of spectral radiance values in a colour image.

4.1 Static simulation

The “rtrace” command (for the rtrace command description see the manual [5]) is used for the Illuminance calculation.

Horizontal grid of 9 points is taken as illuminance sensor.

[Figure 16](#) reveals the homogeneity of the light distribution in the office space if a completely glazed façade with the new angular selective glass is used. The illuminance level is between 100lux and 600lux depending on the sensor distance from the façade.

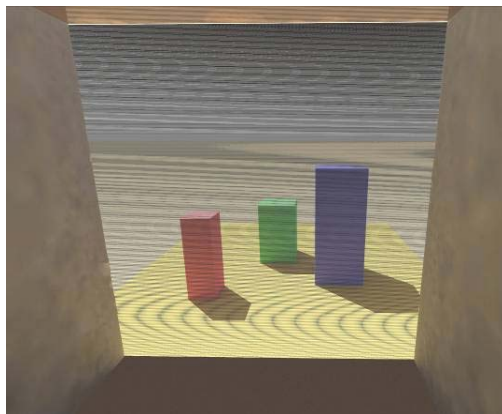


Figure 15: Ximage simulation within Radiance. The simulation are carried out for the 21st June at 10.00am The picture reveals the high transparency of the façade.

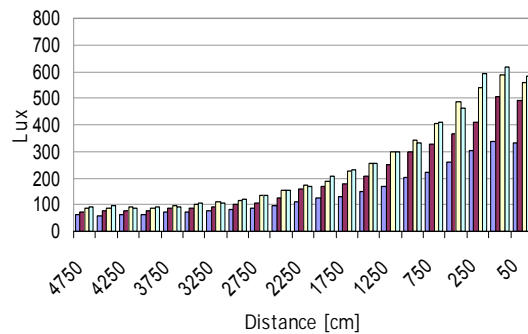


Figure 16: Static simulation: illuminance evaluation for the 21st of June at different hours (from 9.00am, to 12.00am).

4.2 Daylighting availability

The Daylighting availability simulation is done to calculate the benefit of natural lighting inside an office space.

The Daysim software is used.

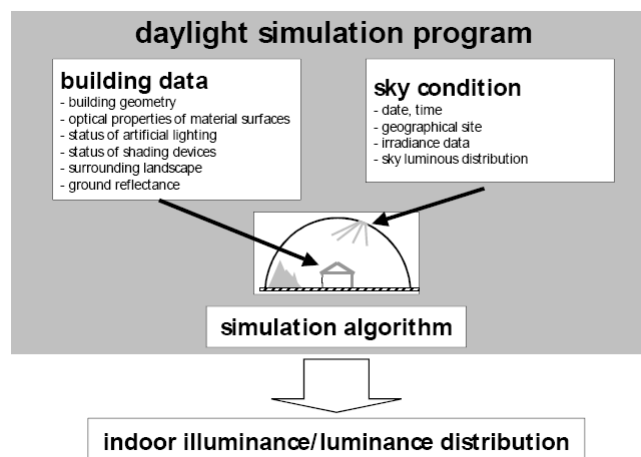


Figure 17: A daylight simulation tool requires information about the building and the prevailing sky conditions to calculate indoor illuminance or luminance distributions.

DAYSIM is a daylighting analysis software package that calculates the annual daylight availability in arbitrary buildings as well as the lighting energy use of automated lighting controls (occupancy sensors, photocells) compared to standard on/off switches. Among the dynamic daylight performance metrics calculated by Daysim are daylight autonomy and useful daylight index.

Different sky definitions for different weather are proposed in the following chapters: Brussels, Freiburg.

A model for a typical office is investigated.

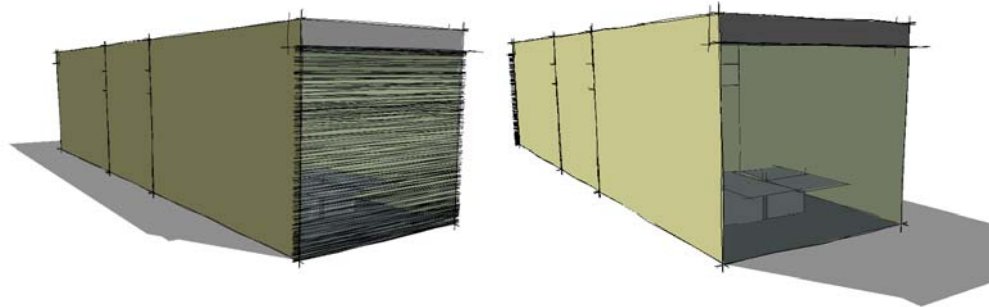


Figure 18: Description of the office model. On the top the South facing façade with angle selective façade, and on the bottom the north facing glazed façade.

Two different geometries ([Figure 19](#)) are considered with different external façade:

- Complete glazed façade with the new angular selective façade
- 70% of the external façade is covered by the new system and the upper part is transparent with horizontal slat to redirect the light

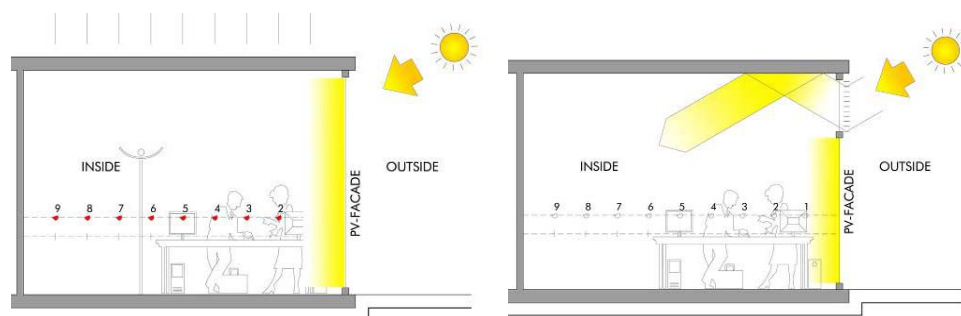


Figure 19: On the left the reference case and on the right the second configuration with external redirecting shading device.

The annual simulations show the good uniformity of the office space illuminance over the whole year.

An annual Daylight Autonomy (DA) calculation is done for quantifying annual daylight saturation and determining the occurrence of direct sunlight. Daylight Autonomy is defined as the percentage of time over a year at which daylight can provide a given illuminance for a given point.

An illuminance of 200lux is taken as minimum value for the analysis (see [Figure 20](#)).

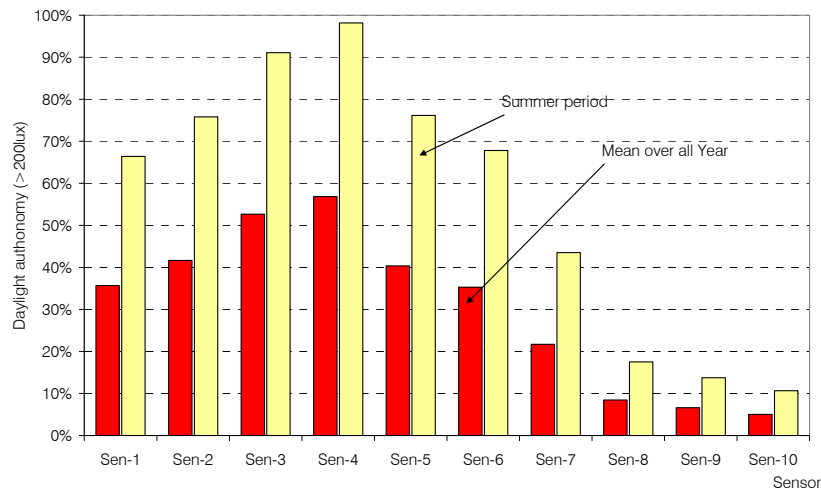


Figure 20: Daylight autonomy (number of hours with more than 200lux) with redirecting venetian blinds installed in the upper part of the external window.

4.3 Glare protection

The Radiance package within the program “Evalglare” (the new method for the Daylight Glare probability DGP is described in [14]) is used to evaluate the glare probability.

Three different simulations are carried out by the author for different sun positions:

- Complete glazed façade with external venetian blind (Design-1).
- Complete glazed façade with the new angular selective façade (Design-2)
- 70% of the external façade is covered by the new system and the upper part is transparent with horizontal slat to redirect the light (Design-3).

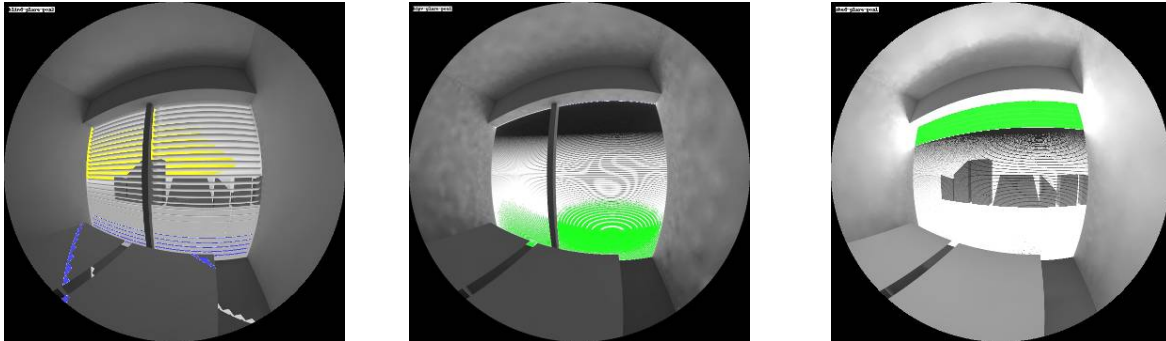
Two different working areas are considered, position one is placed on the desk to the right and position two on the desk on the left of the picture (see [Table 4](#)). The possible glare source areas are underlined with different colours.

Table 4: Three different façades design are simulated. With the Evalglare tool it is possible to evaluate the area of the picture which could be glare source for the user sitting in Position 1 or Position 2. It is important to remember that the colour areas are not 100% glare sources they put in evidence the possible areas of glare.

Design-1

Design-2

Design-3



While the design-1 reveals different glare sources due to the blind position (the slat angle of the blinds is considered fix at 35°) with a critical DGP value (more than 40%), the other two systems have a good glare protection. Especially for the design-2, with a $DGP_2=0,24$, the probable glare source is located in the lower part of the façade (because of the reflection of the external ground) and does not disturb the users.

Also the design-3 with a higher mean luminance than the design-2, has a DGP value acceptable ($DGP_3 < 0.3$).

The DGP analysis reveals the very good glare-protection performance of the new angular selective façade.

4.4 Building energy simulation analysis

The same office, used for the Dynamic Daylight simulations, is used to assess the impact of the new system in building energy simulation, only the external façade of the office 1 (OR1) is designed 90% transparent (with the new system) to increase the influence of using the new angular selective façade instead of a standard double glazing façade with shading device. The new version of the software ESP-r, implemented with the new BlackBoxModel [4] for the evaluation of the total solar energy transmittance of the angle selective façade, is used for this purpose.

The prototype described in the previous part is coupled with a low-e glass pane. A 16mm cavity, filled with gas argon, is placed between the prototype (facing outside) and the low-e glass.

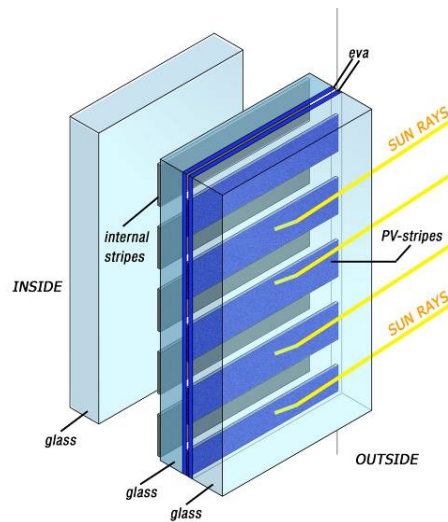


Figure 21: The new system is combined with a low-e glass put in the inside.

Three simulations are carried out to compare the new static system with a glazing façade with external venetian blinds or with internal Genius™ blinds.

The blind slats are tilted depending on the incident solar radiation.

The simulations are carried out during winter period to assess the energy demand for the heating system and during summer period to check the cooling energy demand and the internal comfort.

Further analysis must be done to correlate the solar control properties of the façades with daylight and glare probability. It is obvious that for such static shading systems, like the one proposed by the author, the user can not operate on the daylight level. Only an on-off strategy on the artificial light is considered.

In [Figure 22](#) only the working hours internal temperatures are plotted for the three different façade buildings. It is possible to see the temperature similarity if the new façade is installed or if the façade is with external venetian blinds. As expected the solution with intern Genius blind has a higher temperature for all the summer period.

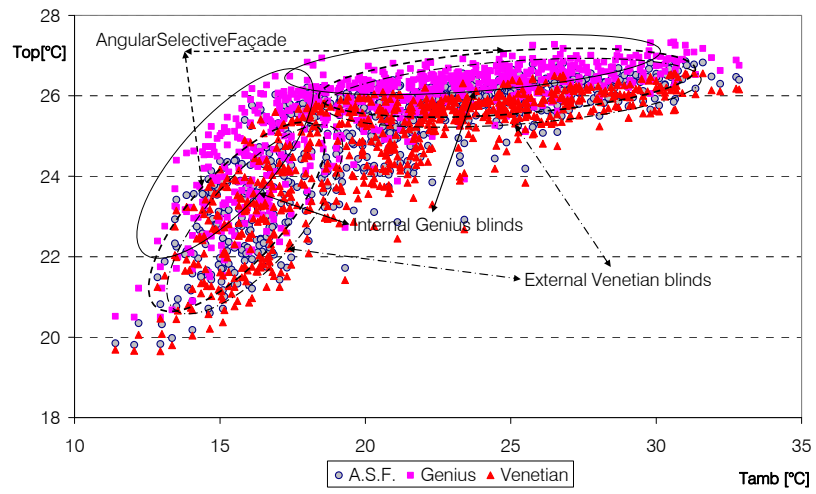


Figure 22: The graph represents the internal comfort depending to the external ambient temperature for the three different façades.

5 PV Integration

The acronym BiPV (Building Integrated Photovoltaics) is used to refer to systems and concepts in which photovoltaic technologies, as well as having the function of producing electricity, also takes on the role of building element. With building elements we mean the parts of the envelope (roof cover, wall facing, glazed surfaces), solar protection devices (sun shadings), additional architectural elements (canopies, balcony parapets, etc.) and any other architectural element necessary for the good functioning of a building (visual and acoustic shielding).

Building Integrate Photovoltaics (BIPV) is today a growing research area. Several technologies are available in the market and new are under development.

5.1 Current available thin-film PV technologies

Three key elements in a solar cell form the basis of its manufacturing technology. The first is the semiconductor, which absorbs light and converts it into electron-hole pairs. The second is the semiconductor junction, which separates the photo-generated carriers (electrons and holes), and the third are the contacts on the front and back of the cell that allows the current to flow to the external circuit. The two main categories of technology are defined by the choice of the semiconductor (see [Figure 23](#)):

- crystalline silicon in a wafer form or
- thin film technology.

The high cost of crystalline silicon wafers (they make up 40-50% of the cost of a finished module) has led the industry to look at cheaper materials to make solar cells.

The selected materials for thin-film technology are all strong light absorbers and only need to be about 1micron thickness, so materials costs are significantly reduced. The most common materials are amorphous silicon (a-Si, or cadmium telluride (CdTe), CIS or CIGS and compound semiconductors like GaAs.

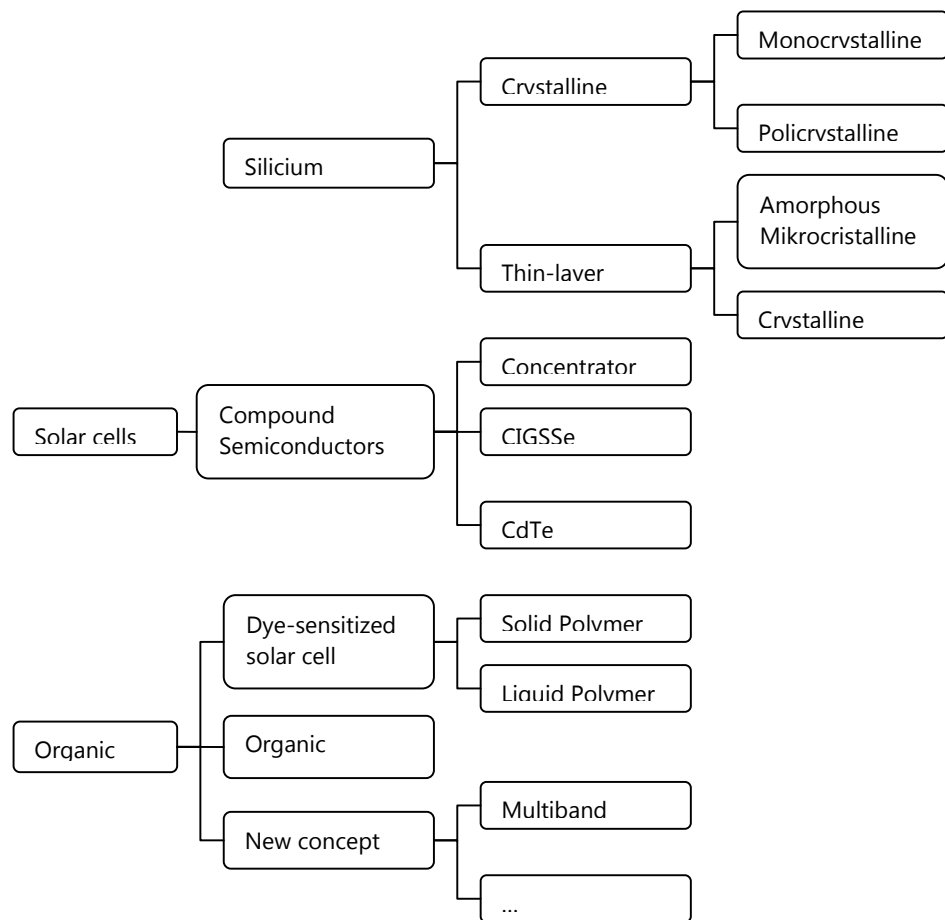


Figure 23 : The scheme represents the current materials for solar cell (Source: OTTI [1]).

Each of these technologies is amenable to large area deposition (on to substrates of a maximum size of 2,6m x 2,2m dimensions) and hence high volume manufacturing. The thin film semiconductor layers are deposited on to either coated glass or stainless steel sheet.

When the photovoltaic module substitutes a glass, semi-transparency is an important factor for the inner well being, either at the light level, thermal contribution and visual contact to the exterior.

BIPV-modules can be inserted for example like double insulated glass ([Figure 24](#)).



Figure 24: The picture on the left shows an example of roof integration. On the right two different solutions for ASI technology (Source: SCHOTT).

5.2 BIPV potentiality

Both the two stripes can be produced with photovoltaic's materials ([Figure 25](#)).

The efficiency of the system strictly depends on the design and on the technology adopted in the construction. The efficiency can be very high if both of the two stripes layers are produced with PV-technologies.

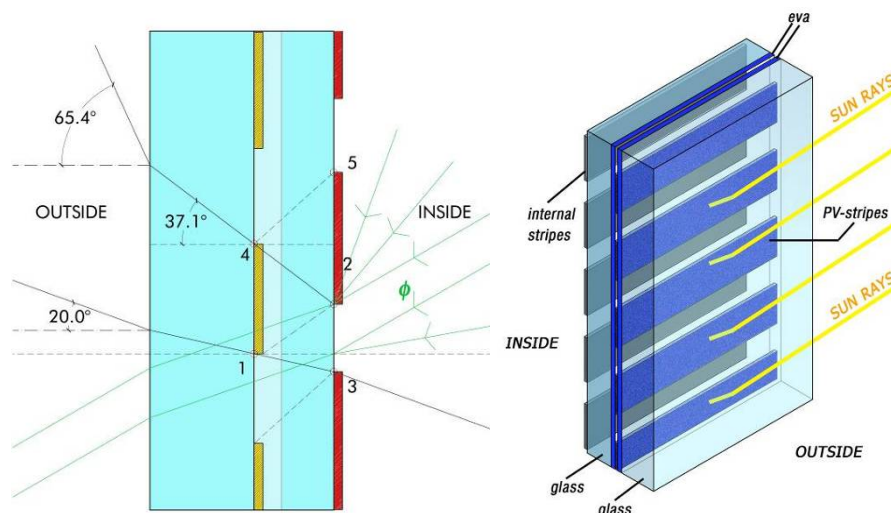


Figure 25: The stripe of the new façade could be produced with photovoltaic technologies.

Three different solutions are here described depending on the pv technologies used and on the position of the solar cells ([Figure 26](#)):

- Solution-1 has only the external layer produced with solar cells. The absorbed light fraction depends on the transparency and the efficiency strictly depends on the adopted PV technology.
- Solution-2 has both layers of stripes made by PV material. The absorbed light fraction increases ideally to a maximum of 96% (if no glass absorption is considered). Two different materials could be used for the two layers of stripe depending on the efficiency that we want to reach and on the shadowing fraction (especially for the inner layer).
- Solution-3 has only the external stripes built up with bi-facial PV technologies. The internal layer of stripes is made with reflective material (e.g. Lambertian reflector) to reflect the incoming light towards the backward face of the external stripes.

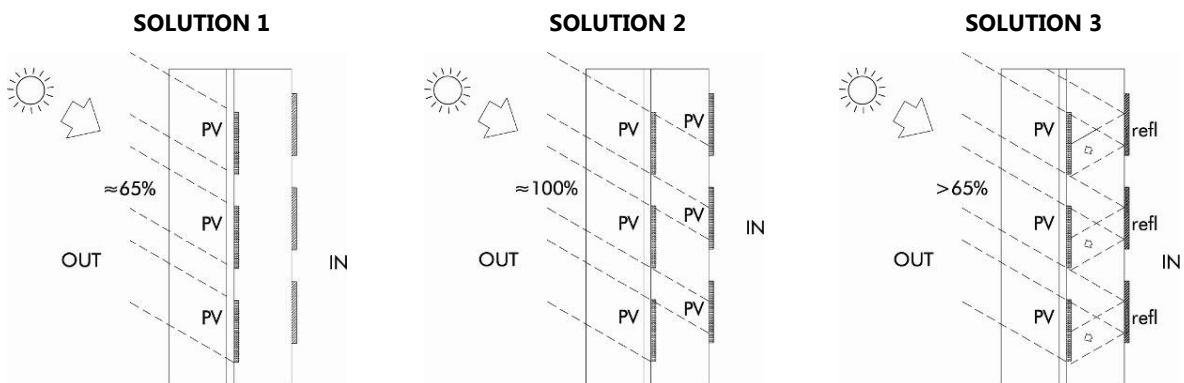


Figure 26: Three solutions are proposed by the author. Different technologies can be used and in different positions.

A first primary evaluation of the efficiency, depending on the incident sun angle (only azimuth 0° is considered), is presented in the following chapter. The evaluation is in the first stage. The presented result must be intended as qualitative results.

5.2.1 First evaluation of the efficiency

The three solutions (A, B, C) have a different light absorption depending on the incident angle. Only direct calculation are done (Figure 27).

The absorption of the external stripes layer depends on the transparent ratio between the external stripes. For that reason the absorption is constant for all the sun altitude angles.

The light reaching the internal stripes depends on the altitude angle and obviously on the design of the façade. The optimized design is here presented (the independent parameters of the façade are equals, $\chi = \alpha = 18^\circ$).

The third line represents the sum of the two layers contribution. It is good to underline that for sun light incident angles between 20° and 65° ($\gamma < \xi < \beta$)

the absorption of the complete system is close to 96%. This is because all the light is caught by the system without letting light passing through (only small reflection occurs). The minimum value for the internal stripes layer is reached when all the light that does not meet the external stripes pass through the system.

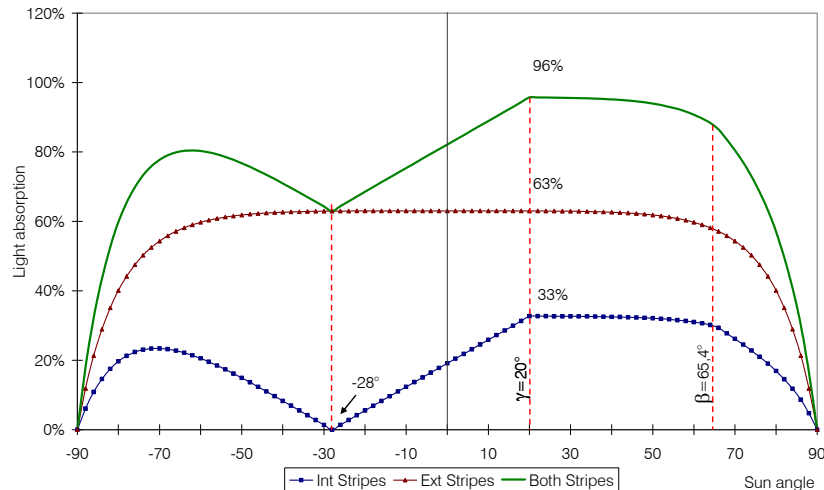


Figure 27: Light Absorption of the two different stripes layer and of the complete system.

The efficiency of the systems is calculated without taking into account the real efficiency of the adopted PV technologies. To leave the study independent from the materials and as general as possible, only the geometry is taken into account and the glass is considered completely transparent (no absorption). In order to be independent from the PV-cell technology used, we calculated the “theoretical efficiency”, which does not take into account the technology-dependent efficiency of the energy conversion in the solar cell. A theoretical efficiency of 100% would mean that the module efficiency would correspond with the maximum efficiency of the respective cell technology.

[Figure 28](#) shows the theoretical efficiency of the three solutions described in [Figure 26](#). The highest theoretical efficiency is reached for solution B where both the stripes layers are with PV technologies.

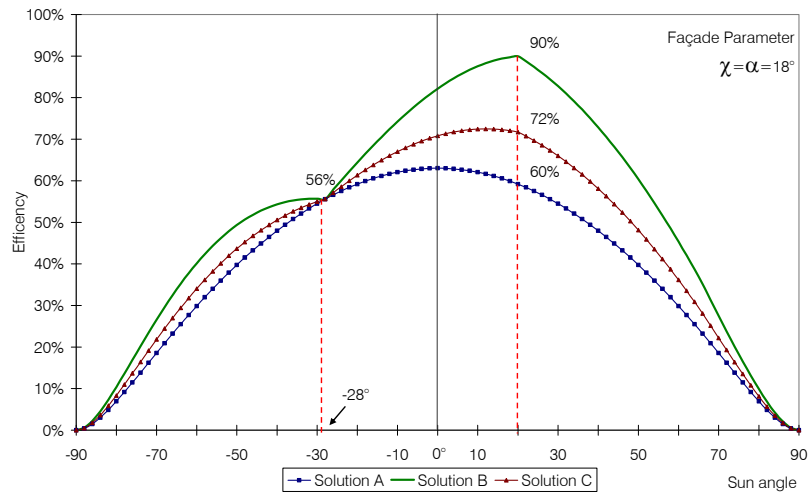


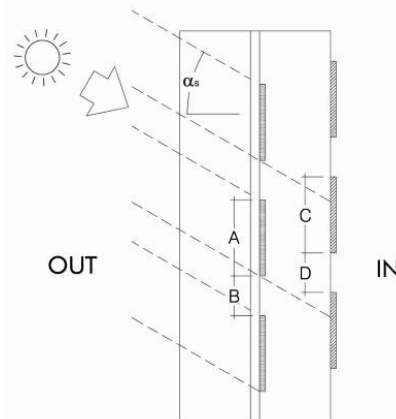
Figure 28: Approximation of the efficiency of the three different solutions. Specific material properties have been neglected.

The lower curve (solution A) is calculated as the fraction between the opaque external stripes and the transparent part of the external façade multiplied by the cosine of the incident angle. The efficiency (ϵ) of the solution B has been estimated to be the cosine of the calculated direct transmission plus the efficiency of the solution A. The bi-facial solution efficiency (solution C) has been estimated as the sum of the efficiency of the solution A and the cosine of the calculated direct transmission reduced by a reflectivity factor (due to the mirror stripes, ρ_{str}) and reduced by the mean efficiency of the back side face of bi-facial PV.

$$\epsilon_{sol_A} = \frac{A}{A+B} \cdot \cos(\alpha_s)$$

$$\epsilon_{sol_B} = \epsilon_{sol_A} + \cos(\alpha_s) [\tau_{vis}]$$

$$\epsilon_{sol_C} = \epsilon_{sol_A} + \cos(\alpha_s) \left[\tau_{vis} \cdot \rho_{str} \cdot \epsilon_{bifac} \cdot \frac{A}{A+B} \right]$$



Where:

$$\rho_{str} = 0,95$$

ϵ_{bifac} is the efficiency of the back face of the bi-facial stripe (external stripes).

6 Façade Integration

In this last section some ideas of building integration are presented.

The new angle selective façade can be used either as stand-alone system for glazing façade (as described in the previous chapters) or as an extra active shading device layer.

In this chapter it is possible to see the good integration of the system either in existing building, just installing the new glass outside the existing windows, or in new buildings.

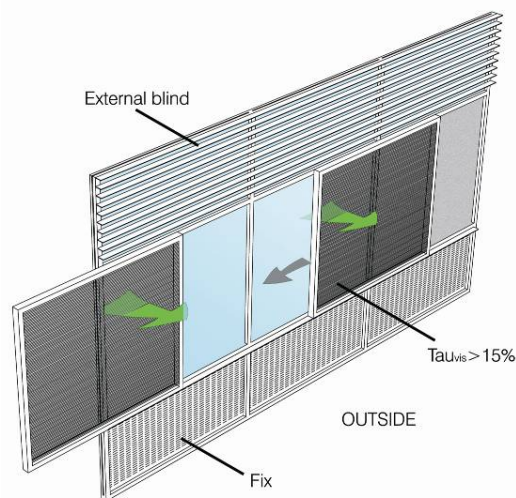


Figure 29:

The picture presents an idea of the integration of the new façade as an extra construction. The external pane can slide among the façade changing the visual and solar transmission depending on the performance the users want to achieve.

The new PV façade can be installed as sliding external shading device to protect, depending on the internal comfort, the office space and the windows (Figure 29).

Especially for open space office or airport hall, the new façade integrated with PV technologies can be installed instead of double or triple clear glazing. If it is coupled with another glass pane and filled in with gas argon the new system has very height performances:

- Low solar transmission (g-value)
- Good visual contact
- Good daylighting
- Electricity production

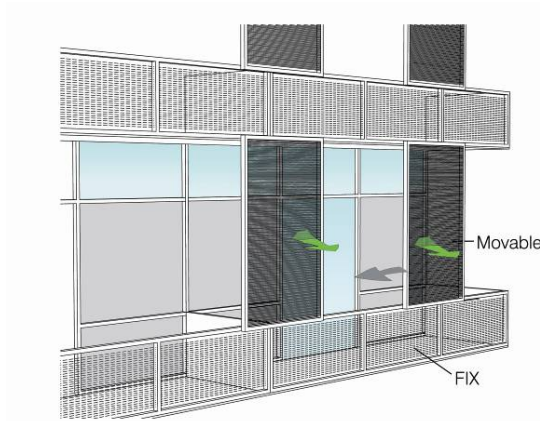


Figure 30:

The picture presents an idea of the integration of the new façade as external shading device. The external pane can slide among the balcony. The user can move it to change the solar protection and the view to the outside.

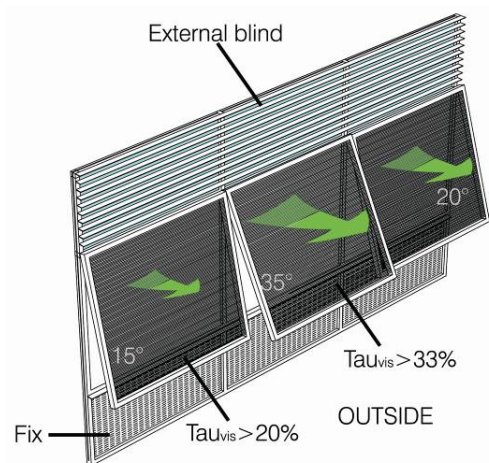


Figure 31:

The picture presents an idea of the integration of the new façade in the normal window. The new window pane can tilt over a certain angle ($>35^\circ$) to change the visual and solar transmission depending on the performance the users want to achieve.

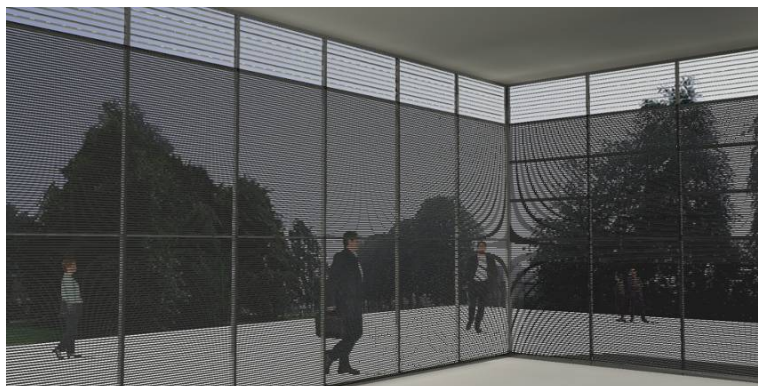


Figure 32:

The new façade can easily installed in airport spaces or big open spaces. The picture shows an example of the façade installed in a complete glazed façade of a big open space (e.g. airport hall).

7 First Prototype

In 2011, before Signet Solar went bankrupt, a fully functional prototypes have been manufactured. The functioning has been proven with lab-measurements (See [Figure 33](#), [Figure 34](#) and [Figure 35](#)).

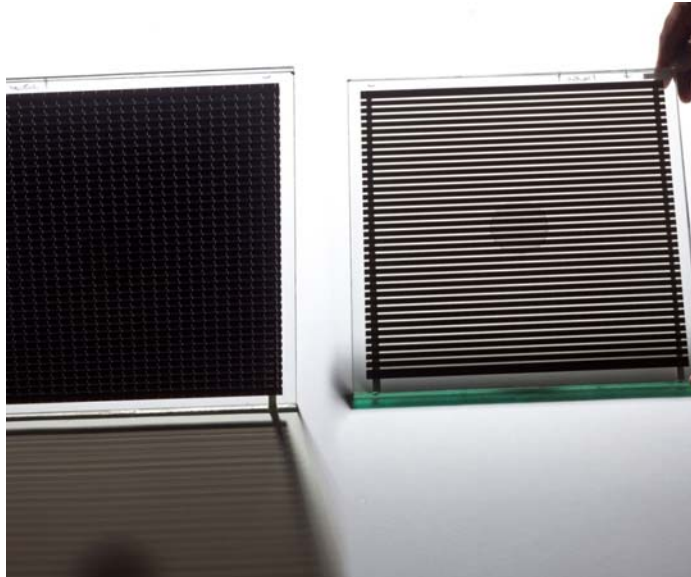


Figure 33: Fully functional BIPV prototype.

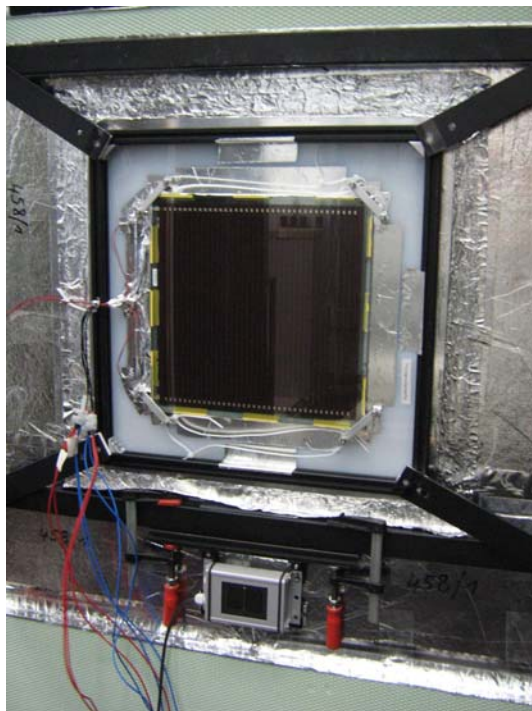


Figure 34: Fully functional BIPV prototype mounted in the test rig at Fraunhofer ISE premises.

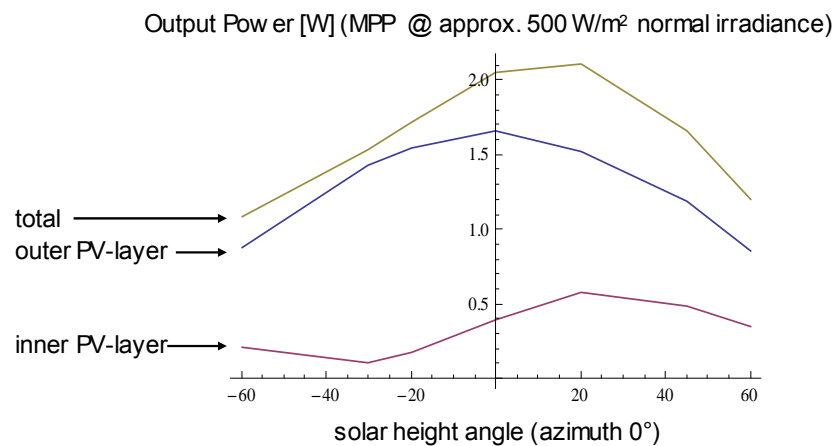


Figure 35: Results of the angle-dependent power output of the module. The angular selectivity is clearly reached. The maximum power-output is provided at (façade-relevant) higher altitude-angles.

8 References

- [1] AA.VV., *Thin Film Photovoltaics –Grundlagenseminar-*, OTTI Training Seminare Tagungen, Würzburg, 2009.
- [2] ESRU 2009, *ESP-r Energy Simulation Program*, available from www.esru.strath.ac.uk
- [3] Frontini F, Brasca M, Aste N., *Design of prismatic pane for daylight control applied to a museum. EuroSun conference. Glasgow 2006.*
- [4] Frontini F., Kuhn T.E., Herkel S., Strachan P., Kokogiannakis G., *Implementation of a new bi-directional solar modelling method for complex façades within the ESP-r building simulation program and its application*, accepted for publication to the 11th International Building Performance Simulation Association Conference and Exhibition in 2009. Glasgow.
- [5] Larson G.W., Shakespeare R., *Rendering with Radiance: the art and science of lighting visualization*. Morgan Kaufmann: San Francisco, 1998.
- [6] Lorenz, A glazing unit for solar control, daylighting and energy conservation. *Solar energy*, 70, 109, 2001.
- [7] Page J.K. and 20 Commission of the European Communities *Prediction of solar radiation on inclined surfaces*. D. Reidel Publishing Co.: Vol. 3, pp. 459.
- [8] Report on the Roadmap for Renewable Energy in Europe, Committee on Industry, Research and Energy, 2007.

- [9] Rosencrantz, T. Angular dependency of optical properties and energy performances of glazing and solar shading devices for windows and façades, pp. 74, 2005.
- [10] Rubin M., Optical properties of soda lime silica glasses, Solar Energy Materials 1985, 12.
- [11] T. Muneer, Solar radiation and daylight models for the energy efficient design of buildings. Architectural press: Oxford, 1997.
- [12] Tsangrassoulis A., A genetic algorithm solution to the design of slat-type shading system. Renewable energy 2006.
- [13] United Nation Environment programme, Buildings and climate change Status, Challenges and Opportunities, 2007.
- [14] Wienold J., Christoffersen J., Evaluation methods and development of a new glare protection model for daylight environments with the use of CCD cameras, Energy and Buildings, 2008.
- [15] *WIS 1.0. and 2.X b-Versions of the Advanced Windows Information System.* WIS Steering Committee coordinated by TNO Building and Construction Research Delft (NL). Distributed by Energy Research Group. University College Dublin. <http://erg.ucd.ie/wis/wis.html>